A Testing Strategy for the Mass Production of CDMS II Detectors

D. Driscoll*, D.S. Akerib*, D. Abrams†, D. Bauer**, P.L. Brink†, B. Cabrera†, J.P. Castle†, C. Chang†, M.B. Crisler‡, R.J. Gaitskell§, J. Hellmig§, S. Kamat*, V. Mandic§, P. Meunier§, T.A. Perera*, M.C. Perillo Isaac§, W. Rau§, T. Saab†, B. Sadoulet§, R.W. Schnee*, D.N. Seitz§, G. Wang* and B. Young¶

*Department of Physics, Case Western Reserve University, Cleveland, OH 44106, USA.
email: ddd3@po.cwru.edu
†Department of Physics, Stanford University, Stanford, CA 94305, USA.
**Department of Physics, University of California, Santa Barbara, CA 93106, USA.
‡Fermi National Accelerator Laboratory, Batavia, IL 60510, USA.
§Center for Particle Astrophysics, University of California, Berkeley, Berkeley, CA 94720, USA.
¶Department of Physics, Santa Clara University, Santa Clara, CA 95053, USA.

Abstract. The Cryogenic Dark Matter Search (CDMS) employs detectors which are capable of simultaneously measuring the ionization and phonon energies deposited by a particle collision. These detectors are 1-cm-thick, 7-cm-diameter crystals of either germanium or silicon with a thin film of aluminum and tungsten patterned on the surface. This presentation discusses the testing regimen that a typical CDMS detector undergoes before it gets approval for final installation at the CDMS II deep site in Soudan, MN which will come online in early 2002. Now that our technology is relatively stable, the main focus of our test facilities is to provide quality control for the mass production of our detectors. First, the critical temperatures of the tungsten and other basic quantities are measured in preparation for iron implantation, which will bring the Tc down to the desired range (70 mK). The same basic measurements are taken again after implantation to assure that the correct Tc was achieved. Finally, a detailed map of energy response as a function of position is made to calibrate residual inhomogeneities across the surface.

INTRODUCTION

A great deal of the thrust of CDMS I has been converging on a stable detector technology. We have recently completed the first data-taking run using these new ZIP (**Z**-sensitive **I**onization and **P**honon) detectors [1]. These detectors are 1-cm-thick, 7-cm-diameter crystals of either germanium or silicon with one face of the detector instrumented to detect ionization energies and the other side instrumented to detect phonon energies. The charge channels are fairly straightforward, but employ new amorphous silicon ionization contacts [2]. The phonon channels consist of a thin film which is patterned to form four quadrants of 1000 tungsten meanders connected in parallel with aluminum fins attached to each meander. This arrangement is called a QET (**Q**uasiparticle Trap Assisted, **E**lectrothermal Feedback, **T**ransition Edge Sensor) [3].

Since we have successfully demostrated that we are capable of producing useable

detectors, our testing strategy has now shifted gears to quality control for the mass-production of CDMS II detectors. We have had relatively little problem with the charge channels, so the focus has turned to the phonon channels. With a maximum CDMS II capacity of 42 detectors (7 towers of 6 detectors each), we have stepped up our testing capacity so that we have two testing facilities (UCB and CWRU) which are each capable of testing 3 detectors simultaneously with a turnaround time on the order of a few weeks.

TESTING STRATEGY

The two main goals of pre-implantation testing are to verify the basic soundness of the device and also to determine the necessary pattern for the iron implantation. First, the charge channels are checked to see if they yield pulses. Next, the basic properties of each of the phonon quadrants are measured: their critical current, and normal and superconducting resistances. Critical current is measured as a function of temperature and the output current is measured as a function of input current [6].

This article will not go into detail on the iron implantation step itself (see ref[4]), but recent developments in the production stage have made the pre-implantation tests more critical in determining the amount of implantation. We had naively been using simple T_c measurements and tuning the implantation to bring that T_c down to the deisred $\approx 70mK$. As is shown below, however, this method is only sensitive to the upper end of the transition. Consequently, we unknowingly lowered the T_c of several devices below the useful bias level because a T_c gradient across the detector had increased the width of our transition. Now we use the data taken from the Critical Current and IbIs measurements of the pre-implantation stage to model the variation of T_c across the detector [5]. We can then use more complex patterns for the implantation to try to bring the detector closer to a uniform distribution.

The bulk of the post-implantation testing is identical to the pre-implanation testing. We retake the T_c, Critical Current, and IbIs measurements as before. The main goal here is to verify that the iron implantation went well and that the detector meets the specifications necessary for running in the experiment. In addition, we uniformly illuminate the detector with a gamma flood source and map the detector response across the surface. By measuring the time delay for the phonon signal to reach each of the four quadrants, we can "triangulate" the location where the interaction occurred. Using the measured energy from the charge channels (we typically use a ^{57}Co source with an easily identifiable 122 keV line), we create a correction matrix for the phonon channels which is used offline to improve the energy resolution. We also install collimated sources (typically ^{241}Am) to directly map *x*-*y* position.

CRITICAL TEMPERATURES AND RESISTANCES

Tungsten has a T_c of 15 mK in the bulk α phase. Thin films of tungsten also contain the β phase, which produces a much higher T_c. This can range as high as 4 K [3] and greatly depends on the method of deposition. Our current method of production using a

Balzers magnetron sputtering system has reliably produced films with $T_c s$ in the range of $90-150\ mK$, and iron implantation can bring that value down to the desired value of $\approx 70mK$ [4].

The critical temperature is measured by putting a minimal amplitude triangle wave across the bias resistor ($20m\Omega$) and reading out the current in the QET with a SQUID array. We start at a high temperature where the sensor is fully normal and then slowly scan down in temperature. Each quadrant of the sensor is composed of 1000 tungsten meanders connected in parallel and hence the resistance of the whole sensor is $\frac{1}{R} = \frac{N_{sc}}{R_{sc}} + \frac{N_{norm}}{R_{norm}}$, where N_i refers to the number of meanders in state i. Each meander has a normal resistance of about 1 $k\Omega$, so when the sensor is fully normal, it has a resistance of 1Ω and the current is then $I_s \approx I\frac{R_B}{R_{TES}} \approx (2\%)I$.

Once a single meander goes superconducting, a kink is seen the the output triangle wave with a steeper slope ($I_s \approx I$) corresponing to the parasitic resistance, typically of order $10m\Omega$. We continue scanning down in temperature until the output wave is completely superconducting. It is hard to judge this point because the resistance has already dropped by 50% after only 10 resistors (1%) have gone superconducting. While this makes the T_c measurement more sensitive to the upper part of the transition, this method of determining transition width indicates the T_c gradient across the whole detector.

The superconducting and normal resistances are basic checks of continuity for the sensor. For example, a shorted meander will show up as a higher R_{sc} and a open meander will show up as a higher R_{norm}.

CRITICAL CURRENT AND IBIS MEASUREMENT

The critical current is simply the minimum input current required to drive the sensor into the transition region for a given temperature. As we have seen above, simply measuring the resistance of the QET is relatively insensitive to how many meanders are superconducting. The critical current, however, can be used to reconstruct this information. Most of the current will be carried through the meanders which are superconducting. The fewer meanders that are superconducting, the more current that each meander must carry. It is a simple matter, then, to approximate the number of superconducting resistors by dividing the sensor critical current by the critical current of a single meander. This assumes a uniform parasitic resistance and critical current for all meanders, but it still makes a fair approximation.

The so-called IbIs measurement is another measurement of output current ($I_s = I_{sensor}$) versus input current ($I_b = I_{bias}$)[6]. We slowly vary the input current from $-2mA$ to $+2mA$ over a time of around 5 min. As we can see in Figure 1, there are three distinct regions: a linear region at large current representing the normal resistance, a linear region at small current representing the superconducting resistance, and a transition region between the two. In the intermediate region, electrothermal feedback (ETF) will keep the sensor biased within the transition [3]. For a perfectly sharp transition, ETF will instantly balance an increased Joule heating from the input current with an increased heat flow to the substrate. We would then see a constant power dissipation curve in that

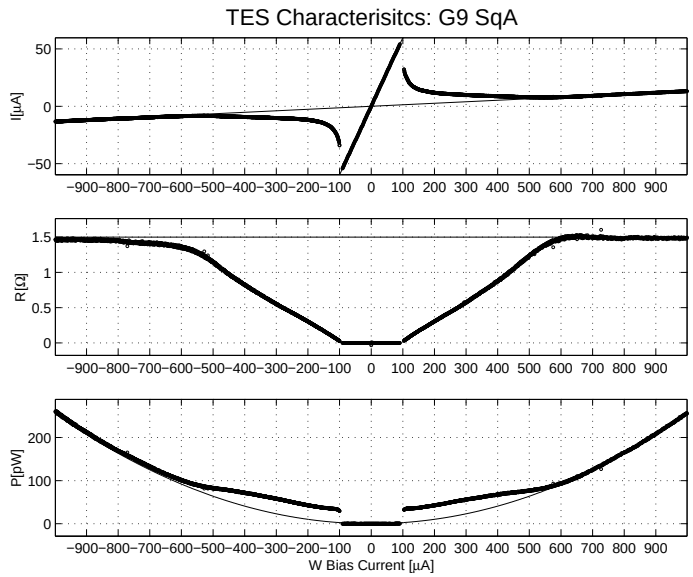

FIGURE 1. A sample IbIs curve for a phonon channel of a germanum ZIP.

region, and from $R = V^2/P$, a resistance that varies quadratically. Our sensors have finite transition widths, which we can measure from the slope of the power dissipation curve in the bias region. Additional features in this region may also indicate that the width of the transition may be due to a T_c gradient across the detector.

CONCLUSION

Now that we have a stable, reliable technology, the main focus of our testing program is to provide quality control for detectors bound for the CDMS II deep site in Soudan, MN, which should be coming online at the beginning of 2002. Our strategy is to determine the basic properties of the detectors and provide data for the iron implantion stage as well as characterizing the energy response in its final state. The test data can also provide feedback for fine-tuning the production steps.

REFERENCES

1. Saab, T., et al., "Demonstration of the CDMSII ZIP technology at a shallow underground site", in *these proceedings*, 2001.
2. Shutt, T., et al., "Amorphous Silicon Ionization Contacts on Germanium and Silicon", in *these proceedings*, 2001.
3. Irwin, K., *Phonon-Mediated Partical Detection Using Superconducting Tungsten Transition-Edge Sensors*, Ph.D. thesis, Stanford University, Stanford, CA 94305 (1995).
4. Young, B., Saab, T., Cabrera, B., Cross, J., Clarke, R., and Abusaidi, R., *Journal of Applied Physics*, **86** (1999).
5. Brink, P., et al., "Determination of the Tc distribution for a 1000 TESs", in *these proceedings*, 2001.
6. Saab, T., *CDMS Note 9911001* (1999).